

A detailed comparison of two continuous GPS carrier-phase time transfer techniques

Jian Yao¹, Ivan Skakun², Zhiheng Jiang³ and Judah Levine¹

¹ Time and Frequency Division and JILA, National Institute of Standards and Technology and University of Colorado Boulder, CO, 80302, USA

² PNT Information and Analysis Center, Central Research Institute of Machine Building, Korolyov City, Russia

³ Bureau International des Poids et Mesures, Pavillon de Breteuil, F-92312, Sèvres Cedex, France

E-mail: jian.yao@nist.gov

Received 27 April 2015, revised 14 August 2015

Accepted for publication 17 August 2015

Published 8 September 2015



Abstract

Global positioning system (GPS) carrier-phase time transfer, as a widely accepted high-precision time transfer method, frequently shows a data-batch boundary discontinuity of up to 1 ns, because of the inconsistency of the phase ambiguities between two consecutive data batches. To eliminate the data-batch boundary discontinuity, several techniques have been proposed in recent years. The question is how much the solutions of these techniques differ from each other and how well the solutions are faithful to clocks. To answer these questions, this paper chooses two techniques to study: revised RINEX-shift (RRS) technique [1, 2], and phase integer common-view (Phase-CV) technique [3]. This paper shows that the time deviation of the difference between the two techniques is below 100 ps, for an averaging time of less than 10 d. Especially, for an averaging time of less than 1 d, the time deviation is less than 30 ps. We also find that both RRS and Phase-CV match TWSTFT (two-way satellite time and frequency transfer) and TWOTFT (two-way optical-fiber time and frequency transfer) quite well. Especially, the difference between RRS/Phase-CV and TWOTFT is less than ± 0.25 ns for more than 20 d, for a baseline of 268 km. These results show that both RRS and Phase-CV agree very well, and they are both faithful to clocks. However, this is based on the assumption that there is no obvious change in the GPS receiver reference time. When there is a sudden change in the reference time, Phase-CV cannot follow the time change. In contrast, RRS still follows the time change and represents the clock well.

Keywords: GPS, Carrier-phase time transfer, boundary discontinuity, revised RINEX-shift, phase integer common-view, two-way satellite time and frequency transfer, two-way optical-fiber time and frequency transfer

(Some figures may appear in colour only in the online journal)

1. Introduction

Global positioning system (GPS) carrier-phase (CP) time transfer is a widely accepted high-precision time transfer method. This method provides much lower short-term noise than other time transfer methods, such as TWSTFT (two-way satellite time and frequency transfer) and GPS common-view (CV) time transfer. TWOTFT (two-way optical-fiber time and frequency transfer), as an emerging time transfer method, can potentially be more precise than GPS CP. However, a

long-distance performance of TWOTFT, such as a transatlantic link, does not exist so far. Thus, GPS CP is and will continue to be one of the mainstream time transfer methods.

Along with the development of GPS CP time transfer method, the problem of data-batch boundary discontinuity attracts a lot of attention [4–8]. The boundary discontinuity can quite seriously affect the long-term (e.g. >1 d) time-transfer result. Studies show that the boundary discontinuity comes from the uncertainty in the phase-ambiguity estimation for each data batch. Fundamentally, this uncertainty further

comes from the code noise, because the code measurements are used to estimate the phase ambiguity [7].

To solve the boundary-discontinuity problem, several techniques have been proposed in recent years [1–3, 9–11]. Each technique gives good results on paper. However, there is little study on the comparison between these techniques. Thus, we have no idea of how large the results of these techniques differ from each other and how well the results are faithful to clocks. This paper focuses on answering these questions. Here, two techniques are chosen for comparison: revised RINEX-shift (RRS) technique [1, 2], and phase integer common-view (Phase-CV) technique [3]. Section II provides the basic principles of these two techniques. Section III first studies the advantages and disadvantages of each technique, and then compares their performance for baselines of 600 km–2500 km, with TWSTFT as a reference. A three-station closure of Phase-CV is also done, to check its self-consistency. Section IV compares the results of these two techniques with a TWSTFT result for a baseline of ~268 km. The comparisons done in sections III and IV make us conclude that both techniques work well for a baseline of no longer than 2500 km. However, this conclusion is true only when there is no change in the GPS receiver reference time. Section V studies the performance of RRS and Phase-CV when the receiver reference time changes. We find that RRS can follow the change, while Phase-CV cannot.

II. Principles of RRS and phase-CV

The RRS is actually an updated version of PPP (precise point positioning). It runs PPP for a data batch of multi-days (here, we choose 10 d) and extracts the middle epoch. Then we take another data batch that starts 10 min later and ends 10 min later than the previous data batch. And we run PPP for this new data batch, and extract the new middle epoch. It does this data-batch shift by 10 min again and again. The solutions at all middle epochs form the RRS result [2]. Here, we should mention, if there is a GPS data anomaly, a program is run to repair the anomaly and the RRS program uses the repaired GPS data [12]. Previous study has shown that the RRS technique can achieve the 10^{-17} level of instability for an averaging time of 20 d with TWSTFT as a reference, while the conventional 30 d PPP processing is still $\sim 2 \times 10^{-16}$ for the same averaging time [2].

Phase-CV is similar to the traditional GPS CV time transfer, but using the phase data rather than the code data. Phase-CV is achieved by two steps. First, it uses PPP to estimate the absolute station coordinates and tropospheric zenith delays (TZD). Second, it does the single-difference of phase measurements between two stations, for the same GPS satellite. The single-difference recovers the integer property of the phase ambiguities. By using the coordinates and TZDs in the first step, we can resolve the integer ambiguities and clock difference between the two stations [3].

III. Comparison between RRS and phase-CV

In this section, we first discuss the advantages and disadvantages of RRS and Phase-CV. Then we compare the technical

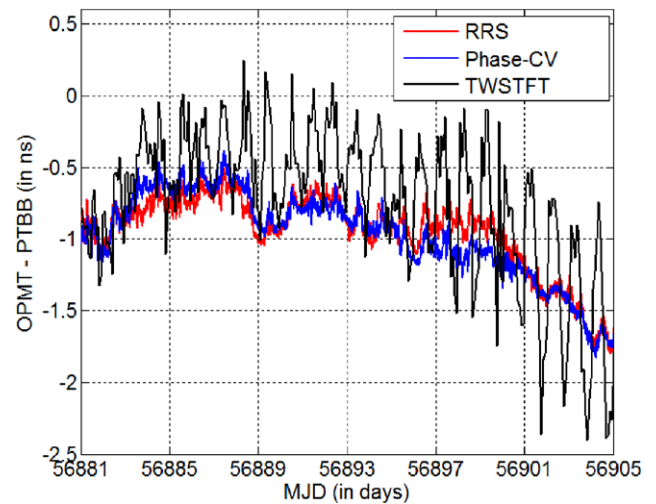


Figure 1. Time comparison between OPMT and PTBB, using RRS, Phase-CV, and TWSTFT. Note, TWSTFT facilities at both OP and PTB share the same reference times as GPS receivers. Slope from the hydrogen maser at OPMT has been removed, and some constant offsets are added to the three curves to overlap each other.

performance of RRS and Phase-CV, for baselines of 600–2500 km. We will see that they agree fairly well.

Before we study the technical performance of each technique in the later part of this section, we here want to address the advantages and disadvantages of each technique. These issues are often ignored, but they can sometimes be even more important than the pure technical performance.

First, RRS requires only a single station [2], while Phase-CV requires two stations [3]. So RRS is still a type of PPP, while Phase-CV is not.

Second, RRS works for any baseline, short or long, since RRS does a time comparison between local time and the IGS (international GNSS service) time. The long-baseline performance of RRS (between NIST and PTB), with respect to TWSTFT, has been shown by figure 11 of [2]. Phase-CV typically works worse as the baseline increases, because of few common-view GPS satellites and no common path [3]. The network processing of Phase-CV, which is still under development, may help the long-baseline performance of Phase-CV.

Third, the solution of RRS is unique, no matter what the start date and the end date are. However, the solution of Phase-CV is not unique. First, it depends on the absolute station position, which can vary by ~1 cm when different GPS data batches are used. Thus, different people may use slightly different positions for Phase-CV. A slightly incorrect absolute position can lead to a small slope in the Phase-CV solution. The absolute position may also change as time passes. Second, Phase-CV is for frequency transfer. In order to achieve time transfer, we need to align the Phase-CV solution with the PPP solution on a long time interval (e.g. >10 d). However, the choice of a long time interval is arbitrary. Different long time intervals (e.g. MJD 56000–56010, or MJD 56001–56015) in PPP can lead to different absolute times in Phase-CV. This can make Phase-CV ambiguous in time transfer.

Fourth, RRS can be affected by the errors from the GPS satellite orbit and clock [2]. Even though IGS has provided

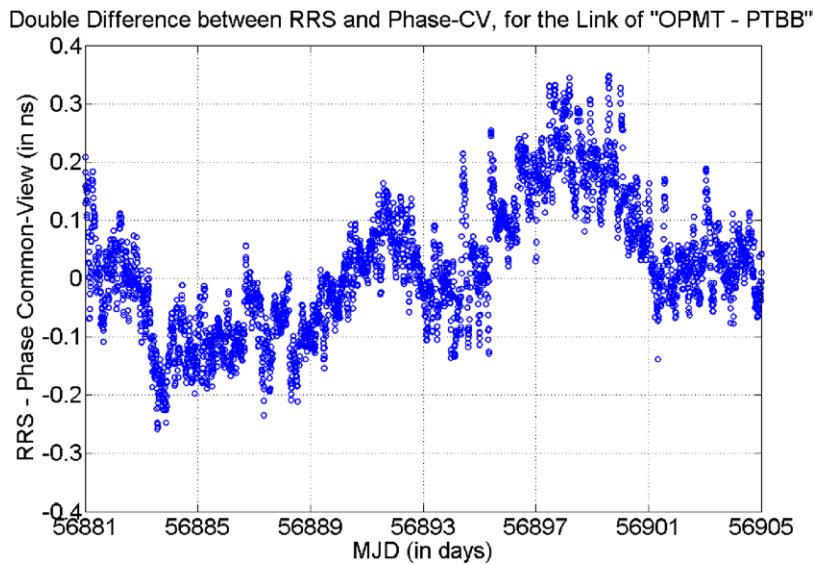


Figure 2. Double difference between RRS and Phase-CV during 56881.0–56905.0, for the link of ‘OPMT-PTBB’.

precise satellite orbit and clock information, there could still be small errors, e.g. a few millimeters. Phase-CV works well in this aspect, because it cancels out the common errors from satellites and path [3]. Besides, Phase-CV is more likely to be insensitive to small noise because of the integer property of the phase ambiguity. For a short baseline (<100 km), broadcast ephemeris can even be used for Phase-CV without too much performance degrading.

Fifth, RRS increases the computation burden quite significantly, although it can be parallelized easily (e.g. one micro-processor core is used to compute MJD 56000.0–56000.25, and another core is used to compute MJD 56000.25–56000.50). Phase-CV requires more computation than PPP, but the increase is not big. Phase-CV is a sequential process.

Sixth, Phase-CV can work in real time or near real time, while RRS cannot. RRS has a latency of 5 d.

Lastly, Phase-CV sometimes cannot keep the integer ambiguity property, which leads to a re-initialization of the processing settings, while RRS does not have this problem.

Now, let’s compare the technical performance of RRS and Phase-CV, for baselines of 600–2500 km.

PTBB is a GPS receiver at PTB (Physikalisch-Technische Bundesanstalt), Germany. The coordinates of this receiver are $X = 3844060.1$ m, $Y = 709661.2$ m, and $Z = 5023129.5$ m, in the ITRF (international terrestrial reference system) coordinate system. The reference time of PTBB is UTC(PTB) with a constant delay. OPMT is a GPS receiver at OP (Paris Observatory), France, with the coordinates of $X = 4202777.4$ m, $Y = 171368.0$ m, and $Z = 4778660.2$ m. The reference time of OPMT comes from a hydrogen maser, which usually has a non-zero slope. We should mention that the TWSTFT facilities at both PTB and OP share the same reference times as the GPS receivers. The baseline of the link of ‘OPMT-PTBB’ is ~692 km.

We do the time comparison between OPMT and PTBB using RRS, Phase-CV, and TWSTFT, for MJD (Modified Julian Date) 56881.0–56905.0 (figure 1). Note, the slope from the hydrogen maser at OP has already been removed and some

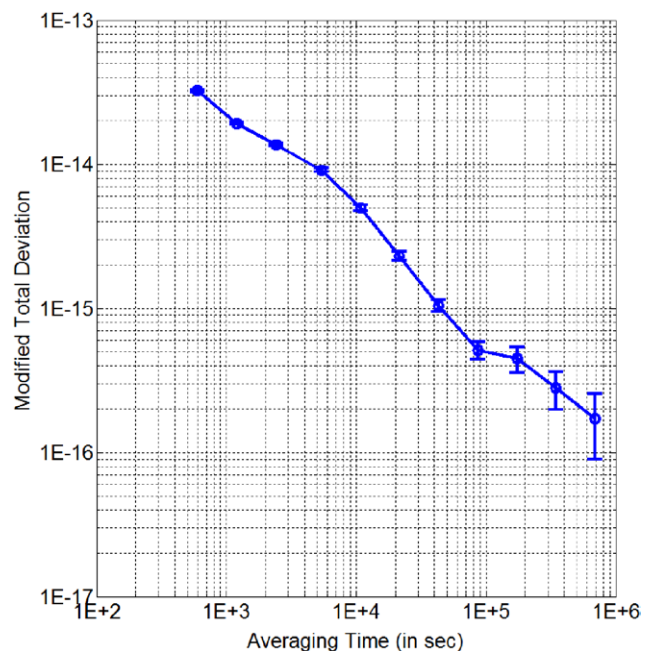


Figure 3. Modified total deviation for the double difference between RRS and Phase-CV, for the link of ‘OPMT-PTBB’.

constant offsets are added to the three curves to overlap each other. Here, we should emphasize that we use exactly the same GPS data of OPMT and PTBB for both RRS and Phase-CV. From figure 1, we can see that both RRS and Phase-CV provide continuous solutions. They match each other very well. They also match the TWSTFT result quite well, although there is an approximately 0.5 ns discrepancy during MJD 56887–56895. This discrepancy could come from either GPS time transfer or TWSTFT or both [13].

To investigate the agreement between RRS and Phase-CV, we do double-difference between RRS and Phase-CV for the link of ‘OPMT-PTBB’ (figure 2). The difference is within ± 200 ps. This indicates a good match between the two techniques. Modified total deviation (figure 3) and time

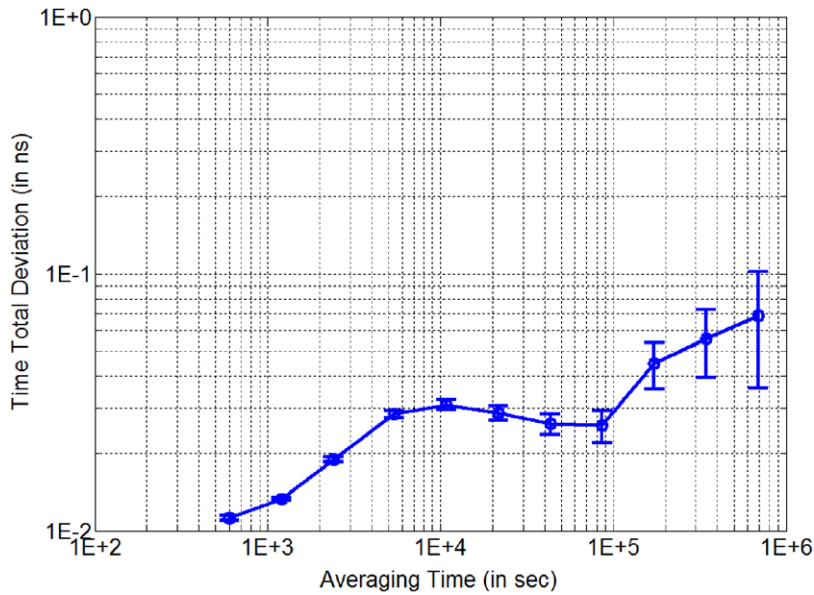


Figure 4. Time total deviation for the double difference between RRS and Phase-CV, for the link of ‘OPMT-PTBB’.

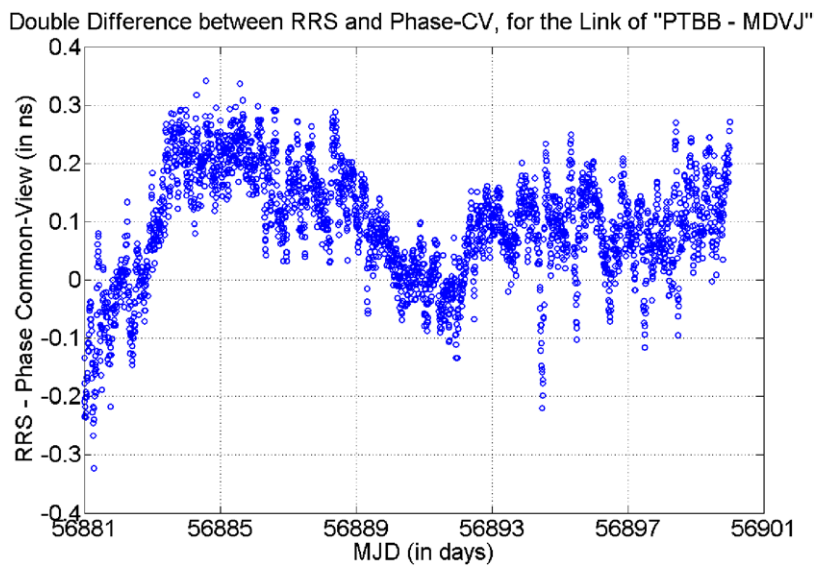


Figure 5. Double difference between RRS and Phase-CV during 56881.0–56900.0, for the link of ‘PTBB-MDVJ’.

total deviation (figure 4) reveal the frequency stability of the double difference between RRS and Phase-CV. From figure 3, we can see that the two techniques match with a fractional uncertainty of $\sim 5 \times 10^{-16}$ for an averaging time of 1 d, and $\sim 2 \times 10^{-16}$ for an averaging time of 10 d. Figure 4 shows that the time deviation of the double difference is below 100 ps for an averaging time of less than 10 d. Especially, the time deviation is less than 30 ps within 1 d. This indicates that even though we process the GPS code and phase data using two different techniques, the time-transfer results are consistent with each other. This validates both techniques.

To further verify the above conclusion that both techniques match each other very well, we also compute the double difference between the two techniques for other baselines.

MDVJ is a GPS receiver in Mendelevo, Russia, with the coordinates of $X = 2845456.3$ m, $Y = 2160954.3$ m, and $Z = 5265993.4$ m. The baseline between PTBB and

MDVJ is approximately 1778 km. And the baseline between OPMT and MDVJ is approximately 2457 km. The double differences between RRS and Phase-CV for these two baselines are shown in figures 5 and 6, respectively. Again, we can see that the fluctuation of the difference between RRS and Phase-CV is within approximately ± 200 ps. Here, we should mention that the Phase-CV has an average offset of about +0.35 ns for the link of ‘OPMT-MDVJ’. This constant offset leads to the curve in figure 6 shifting down by 0.35 ns. The reason for the offset comes from the ambiguity of the absolute time in Phase-CV. Phase-CV itself can only provide the frequency transfer result. To provide the time transfer result, it requires the assistance of the conventional PPP solution. However, the boundary discontinuity in the conventional PPP can lead to a slightly biased time transfer result. That is why Phase-CV is 0.35 ns biased from RRS in figure 6.

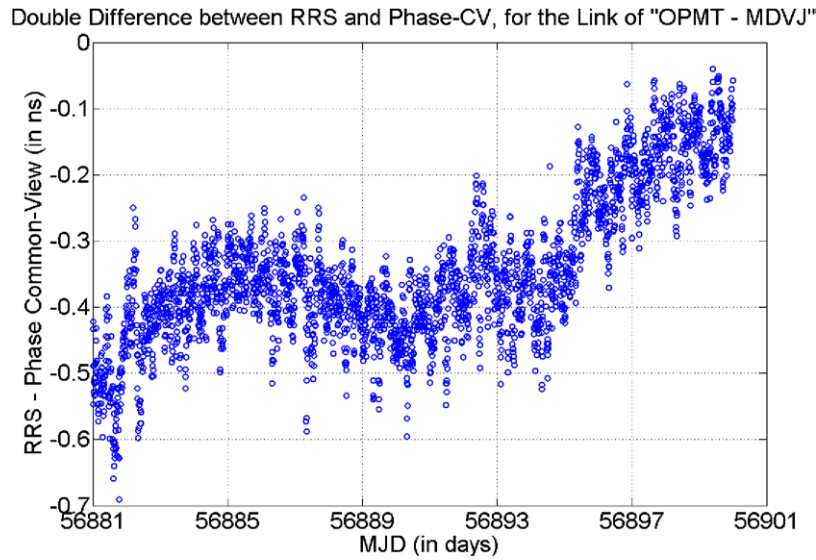


Figure 6. Double difference between RRS and Phase-CV during 56881.0–56900.0, for the link of ‘OPMT-MDVJ’.

From the above discussion, we know that RRS and Phase-CV agree within ± 200 ps, if Phase-CV has the correct initial time. Now that we have done the time transfer between each two of the three stations, a three-station closure may tell us the self-consistency of a time transfer technique. Since RRS is a type of single-point technique, the time difference between two stations is achieved by introducing a common reference time. Often, we choose the IGS time (IGST) as the common reference time. Then, the three-station closure of RRS becomes

$$\begin{aligned}
 \text{Closure} &= (\text{PTBB} - \text{MDVJ}) + (\text{MDVJ} - \text{OPMT}) + (\text{OPMT} - \text{PTBB}) \\
 &= [(\text{PTBB} - \text{IGST}) - (\text{MDVJ} - \text{IGST})] + \\
 &\quad [(\text{MDVJ} - \text{IGST}) - (\text{OPMT} - \text{IGST})] + \\
 &\quad [(\text{OPMT} - \text{IGST}) - (\text{PTBB} - \text{IGST})] \\
 &= [(\text{PTBB} - \text{IGST}) - (\text{PTBB} - \text{IGST})] + \\
 &\quad [(\text{MDVJ} - \text{IGST}) - (\text{MDVJ} - \text{IGST})] + \\
 &\quad [(\text{OPMT} - \text{IGST}) - (\text{OPMT} - \text{IGST})] \\
 &= 0 + 0 + 0 = 0.
 \end{aligned} \tag{1}$$

Equation (1) indicates that the three-station closure of RRS is always exactly 0. The red curve in figure 7 further confirms this conclusion.

However, the Phase-CV is a type of common-view technique. It provides the time difference between two stations directly and no common reference time needs to be introduced in the Phase-CV. Thus, the three-station closure of Phase-CV is

$$\text{Closure} = (\text{PTBB} - \text{MDVJ}) + (\text{MDVJ} - \text{OPMT}) + (\text{OPMT} - \text{PTBB}). \tag{2}$$

Equation (2) cannot be further simplified. Thus, the closure of Phase-CV is not necessary to be exactly 0. The closure test for Phase-CV can show how well it is self-consistent. The black curve in figure 7 shows the result of the Phase-CV three-station closure test. We can see that the closure is not around 0 ns. Instead, it is shifted by approximately -0.37 ns. As mentioned before, this offset comes from the ambiguity of the absolute time in Phase-CV. From figure 7, we know that

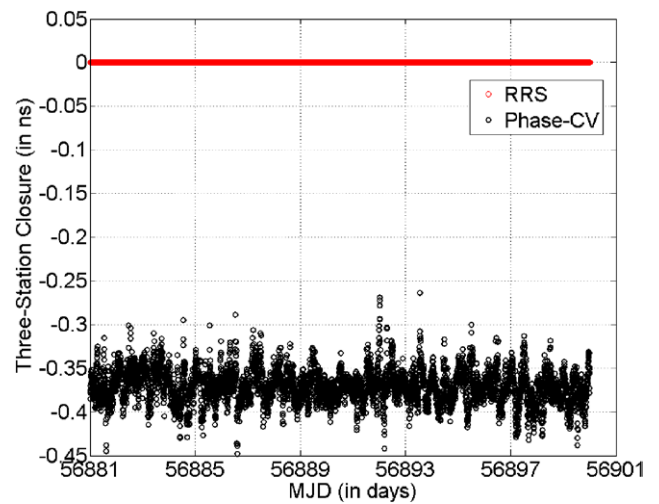


Figure 7. Three-station closure of RRS (red) and Phase-CV (black). The closure is achieved by adding together the links of ‘PTBB-MDVJ,’ ‘MDVJ-OPMT,’ and ‘OPMT-PTBB’.

the peak-to-peak value of the closure is as small as ~ 60 ps. Besides, the closure does not change over time. These indicate that the Phase-CV processing is self-consistent for frequency transfer.

IV. Comparison of RRS and phase-CV with twotft

TWOTFT is a fast-emerging time transfer technique. Many people have demonstrated its ultra-precise time transfer capability [14–16]. Thus, a comparison between GPS and TWOTFT can provide the instability of GPS time transfer, because the instability of TWOTFT is typically smaller or even negligible when compared to GPS.

There is an optical fiber link between AOS (Astrogeodynamical Observatory) and PL (Polish Atomic Time Scale) in Poland [17]. The length of the optical fiber is ~ 420 km. There are also two GPS receivers, i.e. AO_4 and GUM4, at AOS and PL, respectively. The coordinates of AO_4

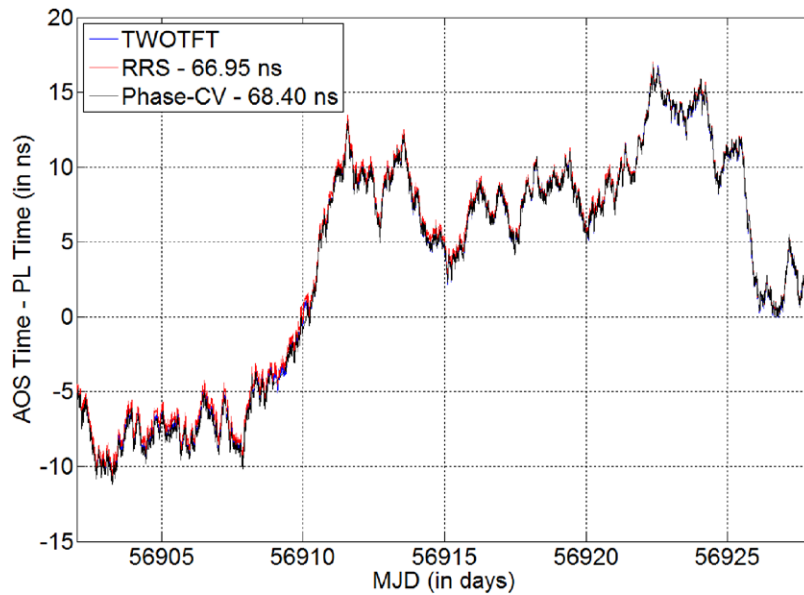


Figure 8. Time difference between AOS and PL using TWOTFT (blue), RRS (red), and Phase-CV (black). The red and black curves are shifted by 66.95 ns and 68.40 ns, respectively, in order to match the blue curve at MJD 56928.0. The blue curve is almost completely covered by the red/black curve. This indicates that RRS and Phase-CV match TWOTFT very well.

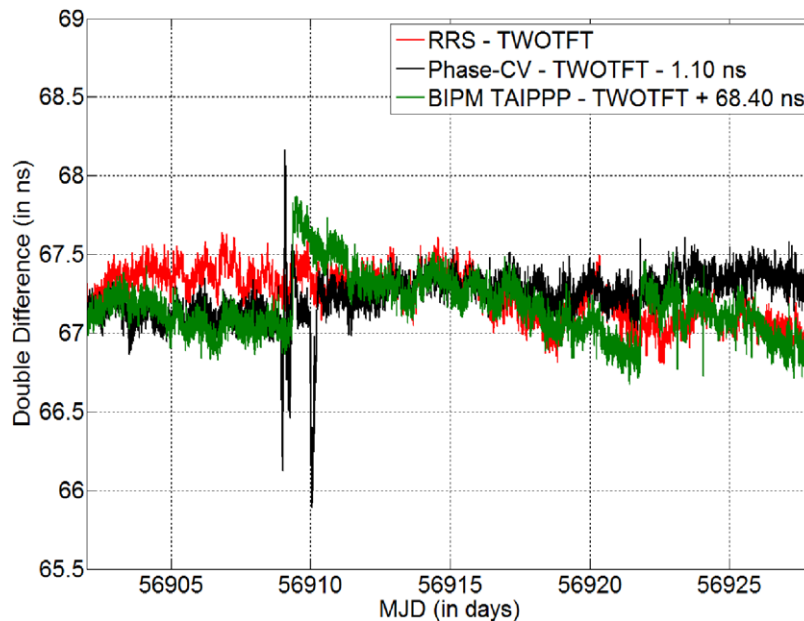


Figure 9. Double differences of ‘RRS—WOTFT’ (red), ‘Phase-CV—TWOTFT’ (black), and ‘BIPM TAIPPP—TWOTFT’ (green), for the link between AOS and PL, during MJD 56902.0–56928.0. (Note, the black curve is shift by -1.10 ns for a better comparison. And the black curve is shifted by $+68.40$ ns, because the BIPM TAIPPP result has already included the delay calibration corrections).

are $X = 3738358.4$ m, $Y = 1148173.7$ m, and $Z = 5021815.8$ m. The coordinates of GUM4 are $X = 3653847.0$ m, $Y = 1402629.2$ m, and $Z = 5019465.1$ m. Thus, the baseline between these two stations is approximately 268 km. The time references for the optical fiber link and the GPS receivers are the same at each station.

Figure 8 shows the time difference between AOS and PL using TWOTFT, RRS, and Phase-CV, for MJD 56902.0–56928.0. We make the three curves match at MJD 56928.0 for a better comparison. The TWOTFT result (blue curve) is hard to see in figure 8, because it is almost completely covered by the red/black curve. This indicates that both

RRS and Phase-CV agree with TWOTFT well over the entire 26 d.

To show the difference between GPS time transfer and TWOTFT, we do double difference between RRS/Phase-CV and TWOTFT (figure 9). The BIPM 35 d PPP (i.e. TAIPPP 35 d) result [18] is also provided in figure 9, as a reference. There are two anomaly points at MJD 56909.35 and MJD 56921.81. The BIPM TAIPPP shows two jumps at both anomaly points. The jumps are 0.7 ns and 0.4 ns, respectively. Because of the jumps, the trend is changed significantly. For example, the time change from 56909 to 56922 is approximately 0.9 ns, which significantly affects the time-comparison result.

In contrast, the RRS technique (red curve) performs very well at both anomaly points. It remains flat (within ± 100 ps) compared to TWOTFT, during 56903–56915. There is also no significant change around the second anomaly point (i.e. during 56921.5–56922.5). Over the whole 26 d, the difference between RRS and TWOTFT is less than ± 250 ps. This indicates the correctness of RRS. The Phase-CV (black curve) does not do well at the first anomaly point. It reinitializes the filter and thus is very noisy during the whole d of MJD 56909. Actually, there was also a jump of about -1 ns on MJD 56909 in the original Phase-CV result, because we need to re-estimate the absolute time using PPP when a re-initialization occurs. We have already removed this jump in figure 9. There was also a jump at the second anomaly point in the original Phase-CV result. We again removed the jump by a simple concatenation. From the black curve, we can see that the difference between Phase-CV and TWOTFT is also less than ± 250 ps. Its slope is pretty small and is not affected by the jumps and the anomaly points. Especially, it keeps flat during 56917–56920, while there is a small dent in RRS. The reason why Phase-CV is so flat probably comes from the fact that Phase-CV uses phase only and thus the noise in code is well excluded. From the above analysis, Phase-CV is good for the frequency transfer. For the time-transfer purpose, a careful calibration or adjustment at each re-initialization point is required in Phase-CV. Next, let's consider the long-term trend of the three curves in figure 9. We can see that both RRS and BIPM TAIPPP go down by ~ 100 ps during the 26 d, while Phase-CV goes up by ~ 300 ps. The increase in Phase-CV is probably because station coordinates were not estimated in the same filter and was fixed for the whole 26 d. Note that the three GPS carrier-phase techniques use the same GPS data, but, unfortunately, the long-term trends are different. This indicates that different GPS CP techniques introduce different long-term trends. And it is hard to tell which technique is more correct. In this case, the long-term difference between RRS and Phase-CV is ~ 400 ps for 26 d, which matches our conclusion in section III that the difference between RRS and Phase-CV is within ± 200 ps.

To study the frequency stabilities of RRS, Phase-CV, and BIPM TAIPPP, with respect to TWOTFT, we compute the modified total deviation of the double difference (figure 10). Note, we have already removed the bad data of Phase-CV on MJD 56909. We can see that Phase-CV provides the smallest instability. RRS is better than BIPM TAIPPP after ~ 6 h. Both RRS and Phase-CV provide $\sim 1 \times 10^{-16}$ level of instability after 5 d. The above results are only based on the fact that the baseline is ~ 268 km. For a transatlantic link, the RRS performance has little change (see figure 4.16 in [19]). However, the Phase-CV performance typically gets worse, if three bridge stations are introduced. We need to have four short baselines (< 2000 km) linked together to achieve the transatlantic time transfer. Thus, the Phase-CV instability for the transatlantic link is increased to double of the instability for a short baseline ($\sqrt{1^2 + 1^2 + 1^2 + 1^2} = 2$). This theoretical frequency instability for a long-distance link is shown by the black dotted curve in figure 10. We can see that RRS becomes the best

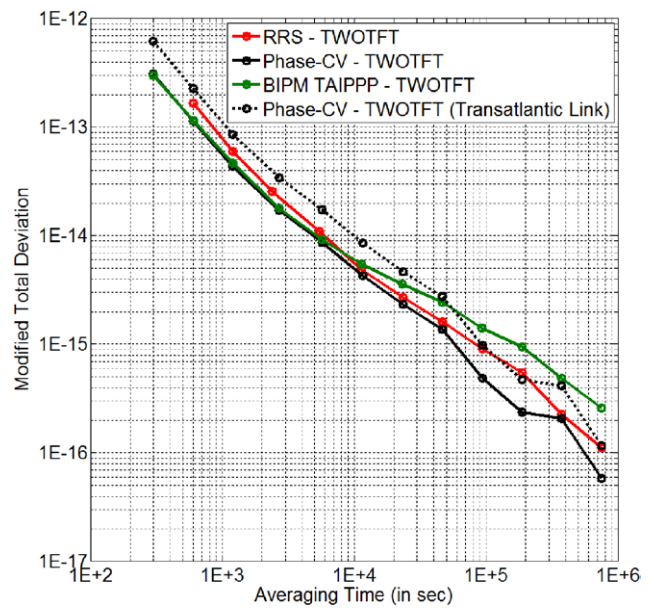


Figure 10. Frequency instability of ‘RRS—TWOTFT’ (red solid), ‘Phase-CV—TWOTFT’ (black solid), and ‘BIPM TAIPPP—TWOTFT’(green solid), for the link between AOS and PL, during MJD 56902.0–56928.0. For a transatlantic link, the theoretical frequency instability of ‘Phase-CV—TWOTFT’ is shown by the black dotted curve. Note, bad data in Phase-CV were already removed for the black solid curve.

among RRS, Phase-CV, and BIPM TAIPPP for the case of a transatlantic link, for an averaging time of greater than 3 h.

The three curves in figure 10 also set the upper limit of the frequency instability of the time transfer techniques. For example, the upper limit of the RRS instability is 5×10^{-15} at 3 h, 9×10^{-16} at 1 d, and 2×10^{-16} at 5 d. The upper limit of Phase-CV instability (for ~ 268 km baseline) is similar to RRS instability, but with a significant improvement at 1 d (i.e. 6×10^{-16}).

In order to improve the performance of RRS, we adjust the weights of code and phase in RRS. The RRS is actually a phase time transfer technique with a long-term steering (e.g. > 1 d) to the code data. Since the code data are noisier than the phase data, we decrease the weight of code in RRS so that the long-term steering is not overreacting. For example, we change the weight ratio of code to phase from the default 1 : 10000 to 1 : 40000. We find that this change makes the dent during MJD 56917–56920 and also other oscillations in the red curve in figure 9 become smaller. Figure 11 shows the RRS result with the improvement of code and phase weights. In terms of frequency stability, there is an improvement for the averaging time of ~ 1 d (see figure 12). Now, the upper limit of the RRS instability becomes 7×10^{-16} at 1 d.

To confirm that the above conclusions are representative for the general case, we do the same comparison among TWOTFT, RRS, Phase-CV, and BIPM TAIPPP, for another time period (i.e. MJD 57070.0–57100.0). During this period, there is no anomalous point. Thus, this is also a good test of the performance of RRS, Phase-CV, and BIPM TAIPPP, when the data are all good. As discussed earlier, we now do not have the re-initialization problem in Phase-CV, because there is no

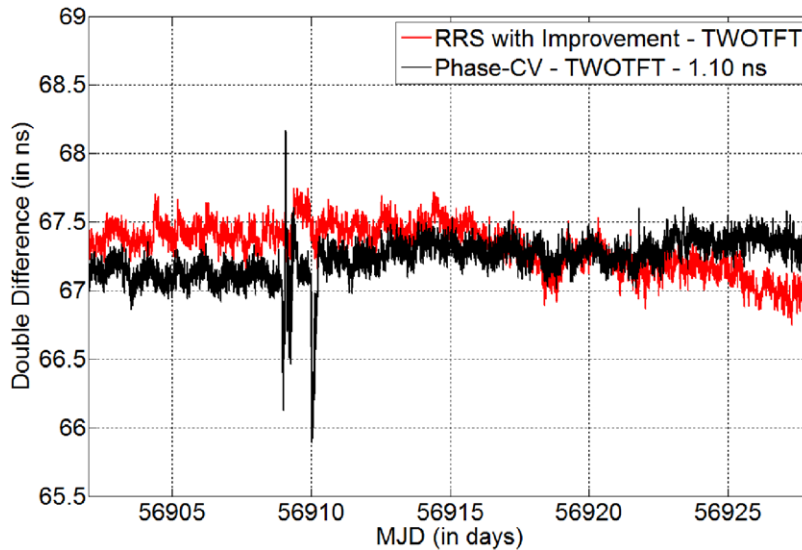


Figure 11. Double differences of ‘RRS with Improvement—TWOTFT’ (red), for the link between AOS and PL, during MJD 56902.0–56928.0. The black curve is the same as figure 9. It is plotted in this figure as a reference.

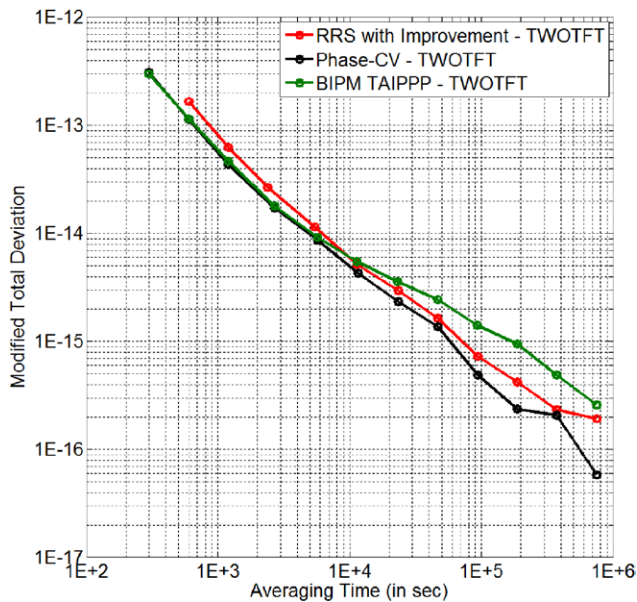


Figure 12. Performance of RRS with improvement in code and phase weights (red curve), for the link between AOS and PL. The black and green curves are the same as figure 10. They are plotted in this figure as a reference.

anomaly. Since BIPM TAIPPP processes ~35 d each time, we have the BIPM TAIPPP results for 57050.0–57081.0 and for 57077.0–57111.0, respectively. Thus, there is a boundary discontinuity between the two data batches. From the green curve in figure 13, we can see that the boundary discontinuity is as big as -2.1 ns. In contrast, the boundary discontinuity is eliminated successfully in the RRS and Phase-CV results (see the red and green curves in figure 13). Similar to our observation in the previous example, the time difference between RRS and TWOTFT varies ± 250 ps during the whole 30 d. We notice that there is an oscillation of ± 250 ps during 57080.0–57086.0 in the red curve. On contrary, although the oscillation in the black curve has a similar pattern to the oscillation in the red curve, the magnitude of the oscillation is obviously

smaller ($\sim \pm 100$ ps). This indicates that Phase-CV matches TWOTFT better than RRS. Similar to the previous example, the frequency stability analysis shows that the Phase-CV instability is $\sim 2 \times 10^{-16}$ at 2 d, while the RRS instability is $\sim 5 \times 10^{-16}$ at 2 d. Because of the big jump in the green curve, the BIPM TAIPPP instability is as big as $\sim 2 \times 10^{-15}$ at 2 d.

Admittedly, both RRS and Phase-CV are still under development and they can be further improved. Nevertheless, even without any further improvement, both techniques are already better than the BIPM TAIPPP, based on the above comparisons with TWOTFT.

V. Response to the reference time change

Based on the above analysis, we have seen that RRS/Phase-CV matches TWSTFT and TWOTFT very well. This demonstrates the correctness of RRS/Phase-CV. However, the analysis is based on the assumption that the reference time for a GPS receiver is stable. For the case of a change in the reference time, we do not know how RRS/Phase-CV responses. The instant response of RRS/Phase-CV is a good test to check if they are faithful to clocks.

At NIST, the reference time for the ‘NIST’ receiver is UTC(NIST). UTC(NIST) is computed as an offset from TA(NIST), the NIST clock-ensemble average time. We observe a small time step of $+455$ ps in the measured value of UTC(NIST) at around 19 : 00 : 00 on MJD 57205, by comparing the measured value of UTC(NIST) with the value expected based on the offset from TA(NIST) (see figure 14). To check if RRS/Phase-CV follows this time step, we compare UTC(NIST) with the AMC2 time using RRS/Phase-CV. AMC2 is a GPS receiver at AMC (Alternate Master Clock in Colorado Springs, Colorado, USA). The physical distance between NIST and AMC is approximately 147 km. The AMC2 time is synchronized with UTC(USNO), within ~ 2 ns. Thus, it is stable and is a good reference for observing the time change in UTC(NIST). From the red curve in figure 15, we

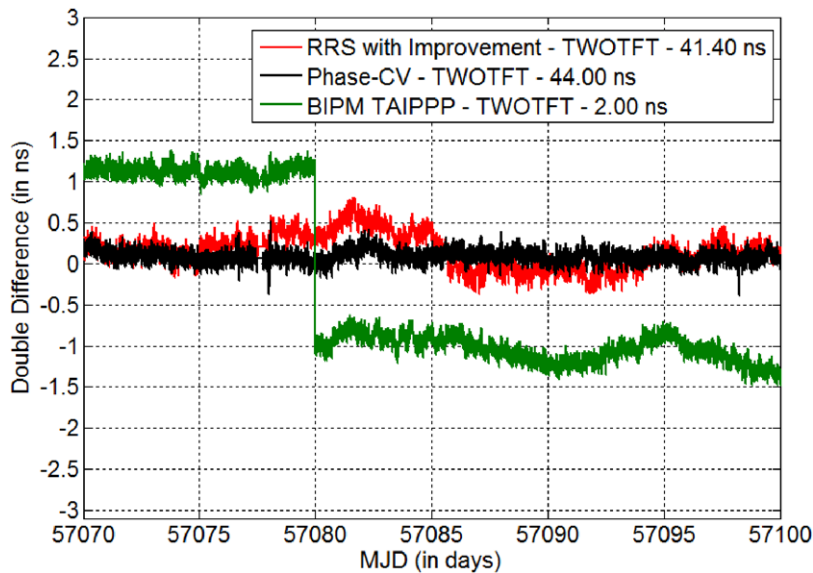


Figure 13. Double differences of ‘RRS—TWOTFT’ (red), ‘Phase-CV—TWOTFT’ (black), and ‘BIPM TAIPPP—TWOTFT’ (green), for the link between AOS and PL, during MJD 57070.0—57100.0. (Note, the constant shifts for the three curves are different from those in figure 9, because the phase stepper at PL was changed in January 2015.)

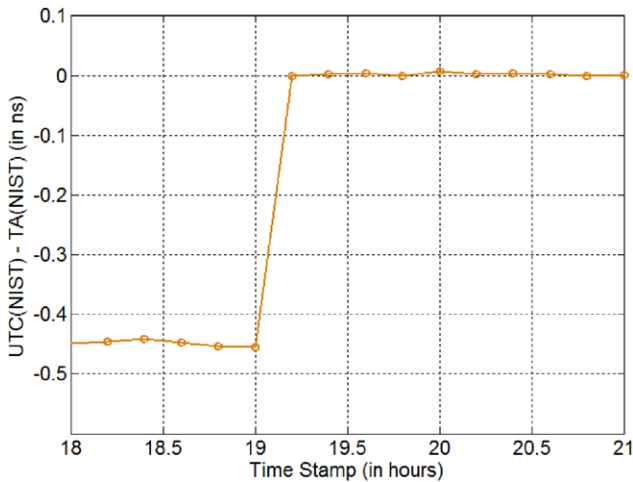


Figure 14. A time step in UTC(NIST) at 19:00:00 on MJD 57205. Here, TA(NIST), the NIST clock-ensemble average time, is used to monitor the time change in UTC(NIST).

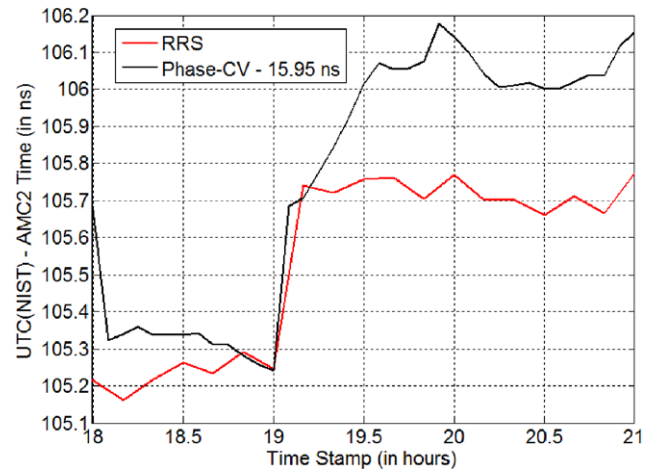


Figure 15. RRS and Phase-CV results at a time step. The time step occurs in UTC(NIST) at 19 : 00 : 00 on MJD 57205.

can see that there is a step of ~ 490 ps at 19 : 00 : 00 in the RRS solution, which matches the time step in figure 14. Although Phase-CV has almost the same time step at 19 : 00 : 00, it starts to walk off afterwards. The walk-off is as big as ~ 500 ps during 19 : 10 : 00–20 : 00 : 00. The Phase-CV solution becomes stable at around 20 : 20 : 00. If we compute the time step from 19 : 00 : 00 to 20 : 20 : 00, we can see that Phase-CV actually shows a step of ~ 750 ps, which is quite different from the measurement result in figure 14. From this example, we can see that RRS can follow the sudden time change, while Phase-CV cannot.

As another example, on the same day (i.e. MJD 57205), we have another time step at 12 : 00 : 00 (figure 16). NIST has two time scales, AT1 and TSC. Before 12 : 00 : 00, TSC was used to generate UTC(NIST). After 14 : 20 : 00, AT1 was used to generate UTC(NIST). Essentially, TSC and AT1 are the same (less than a few hundred picoseconds). However, there is a constant

time difference between the final output of TSC and the final output of AT1, because of different cable delays. This constant time difference leads to the big time step at 12 : 00 : 00 (red curve in figure 16). Unfortunately, this time difference was not monitored on this day. Thus, not like the previous example, we do not have the exact ‘truth’ in this example. Even though, the TWSTFT result is still a good reference to determine whether RRS or Phase-CV represents the time change correctly. Note, we here use the TWSTFT link between NIST and PTB, instead of the link between NIST and AMC. This is because there is no TWSTFT link between NIST and AMC. We know that the PTB time (i.e. UTC(PTB)) is very stable. Thus, the TWSTFT link between NIST and PTB is good to monitor the time change in UTC(NIST). Comparing the three curves in figure 16, we can find that RRS matches TWSTFT quite well. From 8 : 50 : 00 to 22 : 50 : 00, the change in TWSTFT is ~ -6.5 ns and the change in RRS is very similar (i.e. -6.8 ns). The slightly difference between TWSTFT and RRS can come from the diurnal

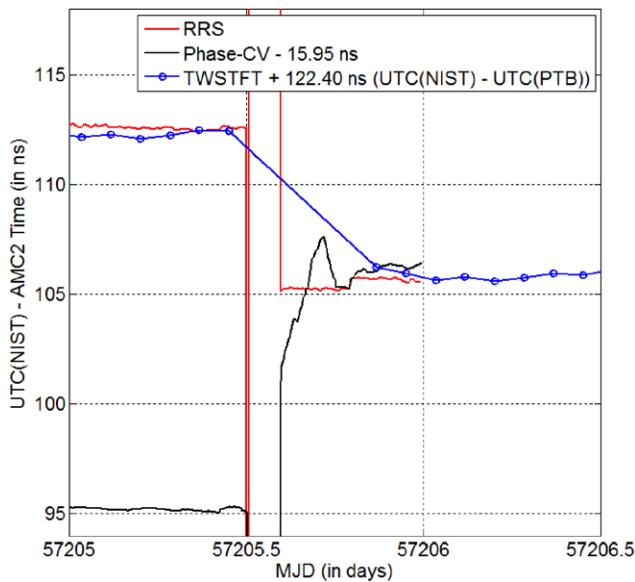


Figure 16. RRS and Phase-CV results at another time step. This time step occurs in UTC(NIST) at $\sim 12:00:00$ on MJD 57205.

effect in TWSTFT or from the GPS measurement noise or something else. After all, they are two different time transfer systems and they could be slightly different as time goes. For the Phase-CV result (black curve in figure 16), however, it does not follow the time change. It increases by $\sim +11$ ns from 8 : 50 : 00 to 22 : 50 : 00, which is completely different from the TWSTFT/RRS result. Besides, it also oscillates significantly (± 2 ns) after the time change. This indicates that Phase-CV is doing something wrong when the time change occurs. There are several reasons that may lead to this behavior in Phase-CV. For example, Phase-CV may re-initialize when there is a reference time change. For another example, the GPS receiver itself may not well follow the time change and thus there are some cycle slips in the phase measurements. This may cause some difficulty in the Phase-CV processing.

In summary, the above two examples illustrate that RRS follows the receiver time change very well. In contrast, Phase-CV, as a frequency-transfer technique, has difficulty in following the time change.

VI. Conclusions

In this paper, we compare two continuous GPS carrier-phase time transfer techniques: revised RINEX-shift (RRS) technique, and phase integer common-view (Phase-CV) technique. The fluctuation of the time difference between these two techniques is typically within ± 200 ps for baselines of less than 2500 km. This indicates a good agreement between the two techniques.

The double difference between these two techniques and other independent time transfer techniques, such as TWSTFT and TWOTFT, can reveal how well the two continuous solutions are faithful to clocks. We find that both RRS and Phase-CV match the long-term trend of TWSTFT quite well. However, RRS and Phase-CV can sometimes walk ~ 0.5 ns away from TWSTFT. This can come from either TWSTFT or

GPS, or even both. Compared with a two-way optical fiber link with a ~ 268 km baseline, both RRS and Phase-CV vary less than ± 250 ps for more than 20 d. This comparison confirms the correctness of both techniques. We find that Phase-CV can provide a better frequency-transfer result than RRS for the averaging time of around 1 d. However, this is only for the case of baseline = 268 km. Its long-distance (e.g. a transatlantic link) performance is unknown (typically worse with bridge stations introduced) and hard to verify, because of no such fiber link. However, a network processing of Phase-CV, which is still under development, may help the long-distance performance. The ambiguity of the absolute time and the problem of re-initialization in the Phase-CV solution also need to be solved, if the time transfer, instead of the frequency transfer, is our main concern. When there is a receiver reference time change, the error of Phase-CV can be as big as a few nano-seconds. Our study also shows that the conventional BIPM TAIPPP can have an incorrect time-transfer slope due to the data-batch boundary discontinuity. With the advent of RRS and Phase-CV, the GPS time transfer becomes more faithful to clocks and thus can observe a remote clock behavior better. Contribution of NIST—not subject to U.S. copyright.

Acknowledgments

The authors thank Francois Lahaye for sharing the NRCan PPP software. Jerzy Nawrocki at AOS, Poland and Albin Czubla at GUM (Electricity Department Central Office of Measures, which is in charge of the Polish Atomic Time Scale), Poland are specially thanked for providing the optical-fiber-link data and the GPS data. We also thank those people who maintain the GPS receivers of NIST, PTBB, OPMT, MDVJ, AMC2, AO_4, and GUM4. IGS is gratefully acknowledged for providing GPS tracking data, station coordinates, and satellite ephemerides.

References

- [1] Yao J and Levine J 2013 A new algorithm to eliminate GPS carrier-phase time transfer boundary discontinuity *Proc. 45th ION PTTI Meeting* pp 292–303
- [2] Yao J and Levine J 2014 An improvement of RINEX-shift algorithm for continuous GPS carrier-phase time transfer *Proc. 27th ION GNSS + 2014 Conf.* pp 1253–60
- [3] Delporte J, Mercier F, Laurichesse D and Galy O 2008 GPS carrier-phase time transfer using single-difference integer ambiguity resolution *Int. J. Navig. Obs.* **2008** 273785
- [4] Defraigne P and Bruyninx C 2007 On the link between GPS pseudorange noise and day-boundary discontinuities in geodetic time transfer solutions *GPS Solut.* **11** 239–49
- [5] Senior K, Powers E and Matsakis D 1999 Attenuating day-boundary discontinuities in GPS carrier-phase time transfer *Proc. 31st PTTI Meeting* pp 481–90
- [6] Guyennon N, Cerretto G, Tavella P and Lahaye F 2009 Further characterization of the time transfer capabilities of precise point positioning (PPP): the sliding batch procedure *IEEE Trans. Ultrason. Ferroelectr. Freq. Control* **56** 1634–41
- [7] Yao J and Levine J 2012 GPS carrier-phase time transfer boundary discontinuity investigation *Proc. 44th PTTI Meeting* pp 317–26

- [8] Weiss M, Yao J and Li J 2012 In search of a new primary GPS receiver for NIST *Proc. 44th PTTI Meeting* pp 179–86
- [9] Petit G, Kanj A, Loyer S, Delporte J, Mercier F and Perosanz F 2015 1×10^{-16} frequency transfer by GPS PPP with integer ambiguity resolution *Metrologia* **52** 301–9
- [10] Dach R, Schildknecht T, Hugentobler U, Bernier L-G and Dudle G 2006 Continuous geodetic time transfer analysis method *IEEE Trans. Ultrason. Ferroelectr. Freq. Control* **53** 1250–9
- [11] Defraigne P, Bruyninx C and Guyennon N 2007 PPP and phase-only GPS time and frequency transfer *Proc. 2007 IEEE IFCS/EFTF Meeting* pp 904–8
- [12] Yao J and Levine J 2014 GPS measurements anomaly and continuous GPS carrier-phase time transfer *Proc. 46th ION PTTI Meeting*
- [13] Zhang V, Parker T and Yao J 2015 Long-term uncertainty in time transfer using GPS and TWSTFT techniques *Proc. 2015 IEEE IFCS/EFTF Meeting* at press
- [14] Ye J et al 2003 Delivery of high-stability optical and microwave frequency standards over an optical fiber network *J. Opt. Soc. Am. B* **20** 1459–67
- [15] Predehl K et al 2012 A 920 kilometer optical fiber link for frequency metrology at the 19th decimal place *Science* **336** 441–4
- [16] Hu L, Wu G, Zhang H and Chen J 2014 A 300 kilometer optical fiber time transfer using bidirectional TDM dissemination *Proc. 46th ION PTTI Meeting* pp 41–4
- [17] Śliwczyński Ł, Krehlik P, Czubla A, Buczek Ł and Lipiński M 2013 Dissemination of time and RF frequency via a stabilized fibre optic link over a distance of 420 km *Metrologia* **50** 133–45
- [18] Petit G and Mercier F 2011 The time stability of PPP links for TAI *Proc. 2011 IEEE IFCS/EFTF Meeting* pp 1041–5
- [19] Yao J 2014 Continuous GPS carrier-phase time transfer *PhD Thesis* University of Colorado at Boulder